Spectrochimica Acta Part B 64 (2009) 974–980

Contents lists available at ScienceDirect

Spectrochimica Acta Part B

journal homepage: www.elsevier.com/locate/sab

Laser-induced breakdown spectroscopy for branching ratio and atomic lifetime measurements in singly-ionized neodymium and gallium ☆

Steven J. Rehse *, Caleb A. Ryder [1]

Department of Physics and Astronomy, Wayne State University, Detroit, MI 48201 USA

ARTICLE INFO

Article history:
Received 26 November 2008
Accepted 22 July 2009
Available online 5 August 2009

Keywords:
Laser-induced breakdown spectroscopy
Neodymium
Gallium
Laboratory astrophysics
Branching ratios

ABSTRACT

Precision laboratory astrophysics measurements can be made in laser-induced plasmas created for laser-induced breakdown spectroscopy. Branching ratios from highly-energetic levels in singly-ionized neodymium may be measured by observing spontaneous emission in laser-induced plasmas in an argon environment at decreased pressures (~7.7 mbar). Utilizing a broadband Èchelle spectrometer with a spectral range from 200–840 nm, the spontaneous emission intensities from hundreds of transitions originating in 138 energy levels in Nd I, Nd II, and Nd III have been observed simultaneously, allowing the determination of branching ratios for these energy levels for branches greater than 1% in the visible wavelength range. In this study, eight branching ratios from the 23,229.991 cm^{-1} level in Nd II were measured and compared to previously determined values as a method for optimizing experimental conditions such as buffer gas pressure and observation delay time. The branching ratios of the eight branches were found to be in excellent agreement with three previously determined values from both experiment and theory. A plan to utilize this laser-induced plasma apparatus to measure the lifetime of the $4s5p\,^3P_2$ level at 118,727.89 cm^{-1} in singly-ionized gallium using a cascade-photon-coincidence method is also presented. Utilizing a solid Ga target ablated in a helium environment, "start photons" at 541.6 nm from a transition into the $4s5p\,^3P_2$ level and "stop photons" at 633.4 nm from a transition out of that Ga II energy level were observed. Single-photon detection will be accomplished using avalanche photodiodes with narrowband interference filters and delay times between the detection of coincident photons from these two transitions will be measured.

1. Introduction

Nucleosynthesis is the method in which nuclides heavier than that of hydrogen are generated in celestial bodies. Neodymium (Nd) is a rare-earth lanthanide metal ($Z=60$) which along with the other lanthanide elements is found in over-abundance (relative to solar abundances) in certain chemically peculiar (CP) stars and old galactic halo stars [1]. Gallium (Ga) is also a heavy element ($Z=31$) found in certain HgMn stars. These heavy elements ($Z>30$) are of significant importance to astrophysicists studying not only galactic elemental abundances, but also stellar age predictions, as well as stellar opacity [2]. Accurate atomic data is absolutely essential for testing models of s-process and r-process nucleosynthesis [3] and to refine our understanding of the radiative, convective, and gravitational processes that determine preferential migration of these elements from the core to the surface [4–6]. Uncertainties in stellar abundances can be large. In fact, the uncertainty in the gallium abundance in the HgMn stars is so large that it has been coined the "Gallium Problem" by Dworetsky [7] and it will remain unresolved until accurate atomic data can be provided.

The most significant hindrance to astrophysicists in this area of research is poor accuracy of atomic data leading to poor calculations in age determinations and over-abundances in CP stars [8]; thus, the need for accurate atomic data by astronomers and astrophysicists [9]. The focus of laboratory astrophysics is to measure atomic properties of atoms and ions that are of interest to observational astronomers. In particular, accurate branching fractions (or branching ratios), atomic lifetimes, oscillator strengths, hyperfine constants, and isotope shifts of both neutral atoms and multiply-ionized atomic species are studied. The present work confines itself solely to the use of laser-induced plasmas to measure branching ratios (BRs) and lifetimes in singly-ionized species.

In an environment free from external interactions such as collisional depopulations, excited atomic energy states must decay radiatively to a lower state via an allowed transition. The probability of a transition decaying through a specific single branch of the many

☆ This paper was presented at the 5th International Conference on Laser-Induced Breakdown Spectroscopy (LIBS 2008), held in Berlin, Adlershof, Germany, 22–26 September 2008, and is published in the Special Issue of Spectrochimica Acta Part B, dedicated to that conference.

* Corresponding author. Tel.: +1 313 577 2411; fax: +1 313 577 3932.
E-mail addresses: rehse@wayne.edu (S.J. Rehse), caleb20k@wayne.edu (C.A. Ryder).
[1] Fax: +1 313 577 3932.

0584-8547/$ – see front matter © 2009 Elsevier B.V. All rights reserved.
doi:10.1016/j.sab.2009.07.024

allowed transitions is defined as a branching ratio. The sum of all branching ratios from a given energy level must equal one. The branching ratios for emission lines can be calculated using Eq. (1)

$$\beta_{ji} = A_{ji} \Big/ \sum A_{ji} = I_{ji} \Big/ \sum I_{ji} \tag{1}$$

where β_{ji} is the branching ratio or transition probability of a given transition from an exited state, j, to a lower level, i, A_{ji} is the Einstein A-coefficient for spontaneous emission from j to i which is the rate of that transition, and I_{ji} is the observed emission intensity from that transition. Thus a careful determination of the emission intensities of all transitions out of a given energy level allows calculation of the branching ratios for all of those observed transitions.

An atomic lifetime is approximately the amount of time an atom spends in a given atomic level before spontaneously decaying to another level, but is more appropriately defined as the inverse of the sum of the rates of all spontaneous transitions from the level. The lifetime is given by

$$\tau_k^{-1} = \sum_i A_{ki} \tag{2}$$

where A_{ki} is the Einstein A-coefficient for spontaneous emission from level k to i. A_{ki} is given by

$$A_{ki}(s^{-1}) = \frac{2\pi e^2}{m_e c \varepsilon_0 \lambda^2} \cdot \frac{g_i}{g_k} \cdot f_{ik} = \frac{6.67 \times 10^{-5}}{\lambda^2} \cdot \frac{g_i}{g_k} \cdot f_{ik} \tag{3}$$

where g_i is the multiplicity of level i, f_{ik} is the absorption oscillator strength from a lower level i to an upper level k, and λ is the wavelength in Angstroms of the transition [10]. In practice, branching ratios defined by Eq. (1) and lifetimes defined by Eq. (2), whether obtained experimentally or via calculation, are combined to calculate absolute oscillator strengths (or transition probabilities) using Eq. (3). Although the absorption oscillator strength f_{ik} is determined, the property desired by observational astronomers is typically reported as the "log(gf)" value of the transition.

Experimentally, lifetimes and branching ratios in ions can be determined via multiple methods which can excite the necessary atomic transitions. Branching ratios are most frequently measured with fast ion beam-laser beam measurements [11] or Fourier Transform Spectroscopy (FTS) methods made with hollow cathode discharge tubes [12]. A large variety of techniques have been developed and utilized for lifetime measurements in the nanosecond region. Among these, fast ion beam-laser technique (FIBLAS) and time-resolved beam-foil spectroscopy (BFS) are common. Other methods for determination of ns lifetimes are based on different kinds of techniques, some using laser-induced plasmas and laser-induced fluorescence techniques (LIF). In such measurements, the laser-induced plasma serves as an ion source characterized generally by a high temperature (~10,000 K), electron density, and ionization degree. The present work incorporates laser-induced breakdown spectroscopy to measure emission intensities for branching ratio determination [13].

Previous work shows laser-induced plasmas can be used as a practical method to obtain atomic data with improved accuracies for calculations. In 1997, Gonzalez et al. studied transition probabilities in Sn–Sb alloys with Sb content lower than 2%, so as to achieve optical thinness in the plasma [14]. They reported data with improved accuracies compared to previous studies in Sb. Later, Rojas et al. measured Sb III branching ratios in laser-induced plasmas. [15] In 2001, Biémont et al. studied atomic lifetimes in eight energy levels of Pr III which previously had never been determined [16]. In 2005, Campos et al. used a laser-produced plasma as a source of Ag ions to study atomic transitions in Ag II. Transition probabilities were obtained from a combination of theoretical lifetimes and experimental branching fractions and presented with comparison to theoretical expectations; which were found to be in agreement within experimental limits [17]. Recently, Xu et al. have utilized laser-induced plasmas to obtain branching ratios in Cd I and Cd II [18] and Ortiz et al. have measured transition probabilities in transitions observed in laser-induced plasmas of Cd II and Zr III [13].

Atomic data for lanthanides is frequently acquired from methods which do not incorporate laser-induced plasmas. Nd II was studied by Den Hartog et al. in 2003, in which atomic data determined with accuracies better than 5% were reported [19]. In this research, over 700 lines were resolved and a collection of transition probabilities were presented from experimentally determined branching ratios and atomic lifetimes using laser-induced fluorescence. Radiative lifetimes of two levels in Ce I, eight levels in Ce II, and nine levels in Ce III were measured by Li et al. at Lund University in Sweden, in 2003, using the time-resolved laser-induced fluorescence technique [20]. Transition probabilities for Ce III were obtained from branching fractions and experimental lifetimes. Spectral lines of Ce III were identified in the spectrum of the magnetic chemically peculiar star α^2CVn and the abundance of cerium was determined to be 800 times greater than that of the sun. In 2007, one of the authors, along with Li et al., measured branching ratios of 46 levels in Nd II using laser-induced fluorescence (LIF) at the University of Western Ontario in Canada [4]. Along with previously determined lifetimes, transition probabilities and oscillator strengths were presented for 430 transitions.

In this study, branching ratios from the 23,229.991 cm^{-1} level in Nd II have been determined and compared to previously determined values as a method for optimizing laser-induced plasma parameters. This level has eight spontaneously decaying branches from 430 nm to 636 nm. Absolute emission intensities for these eight transitions were measured to determine branching ratios for comparison with previous studies using alternate methods and ion sources [4,11,19]. Using lifetimes determined experimentally by others, oscillator strengths were determined. Lastly, we will present initial results indicating the usefulness of a laser-induced plasma as a source of Ga II ions for measuring the lifetime of the $4s5p^3P_2$ level at 118,727.89 cm^{-1} in singly-ionized gallium utilizing a cascade-photon-coincidence technique. Due to its high excitation energy, this lifetime has never been measured by any method.

2. Experimental

The LIBS experimental setup used to make branching ratio measurements is shown schematically in Fig. 1. The laser source is a Nd:YAG laser (Spectra Physics, LAB-150-10) firing 10 ns laser pulses at 10 Hz and operating at its fundamental frequency of 1064 nm to ablate the target, a solid cylinder of Nd (99.99%). The laser pulse energy was 18 mJ/pulse. A 75 mm diameter lens with effective focal length of 18.5 cm was used to focus the laser beam downward into the ablation chamber and incident upon the top side of a rotating Nd sample.

The ablation chamber was a cubical stainless steel container with volume of 3500 cm^3 with a 15.24 cm circular flange on every side for easy accessibility. The chamber was evacuated by a mechanical vacuum pump (Varian DS-302) to achieve an ambient gas pressure of ~7.7 mbar [11] with an argon buffer gas to help create optimal plasma conditions for atomic emission. When using pressures lower than atmosphere, argon buffer gas produces the highest plasma temperature, highest electron density, and highest emission intensity as compared to such gases as helium or nitrogen [21]. The argon buffer gas was introduced via short bursts from a needle-valve and the pressure was monitored by a convection module pressure gauge (Kurt J. Lesker 300-series) capable of detecting pressure ranges from 10^{-4} mbar to 13.33 bar. The sample to be ablated was mounted to one side flange of the cube. An orthogonal flange had a 3.8 cm quartz

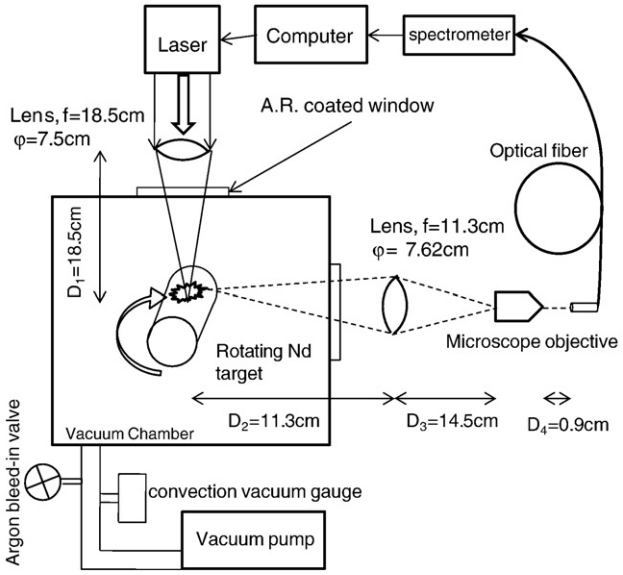

Fig. 1. The LIBS experimental setup used to make neodymium branching ratio measurements. A side-view of the apparatus is shown. The path of the infrared Nd:YAG laser coming through the top of the vacuum cube is depicted with an arrow and solid lines. Visible wavelength plasma emission is collected through a quartz side window and is depicted with dotted lines. The chamber is typically held at argon pressures ranging from 1–15 mbar.

window for transmitting the emitted light from the plasma. This emission was collected by a condenser lens of diameter 7.62 cm and effective focal length of 11.3 cm, located 24.5 cm from the ablation site and 13.5 cm from the quartz window. The light collection optical axis was orthogonal to the incident laser beam axis.

Following the condenser lens was a 20× microscope objective at a distance of 14.5 cm. This microscope objective had an aperture of 8 mm, an effective focal length of 10 mm, a numerical aperture of 0.4 and a working distance of 6 mm. The microscope objective was used to focus the emitted light into a 1-m steel encased multimode optical fiber (diameter = 600 μm, N.A. = 0.22). This fiber transmitted plasma emission to an Èchelle spectrometer with an intensified CCD-array (LLA Instruments, Inc., ESA3000) of 1024 × 1024 pixels (24 μm × 24 μm pixel area). The spectrometer had a useful spectral range of 200 to 780 nm and a resolution of 0.005 nm per pixel in the UV. The instrument-limited full width at half-maximum for peaks in the near-UV was approximately 0.03 nm. A PC equipped with software for operating the pulsed-laser and the gating of the spectrometer ICCD was used.

Emission spectra were obtained with an ICCD open-gate duration of 1 μs, and a gate delay time of 600 ns after the laser pulse. These times were chosen for optimum plasma emission characteristics, including signal-to-noise ratio and integrated signal intensity, yielding atomic data comparable with previous studies. Determination of the 600 ns optimum delay time was one of the results of this study, as will be described in the Results section. Accumulations of 5 integrated laser pulses were averaged together on the CCD chip prior to read-out to achieve an averaged emission to improve signal-to-noise. Each averaged CCD image was then integrated with another 10 separate spectra and the resulting emission spectrum was comprised of a total of 50 spectra.

3. Results

A LIBS spectrum of the rotating Nd target ablated in 7.7 mbar of argon is shown in Fig. 2. The emission spectrum from 200–780 nm is shown. Nd II (as well as most lanthanides) has the majority of its emission lines in the visible range from 375 nm to 550 nm, making it an ideal spectroscopic species. The inset in Fig. 2 shows a zoomed in detail of the spectrum in the vicinity of the 430.357 nm line, the strongest branch from the 23,229.991 cm^{-1} level studied in this work. This branch, as well as most other branches in the spectrum, was easily resolved and experienced no line-blending. Intensities were obtained by fitting the spectrally-corrected background-subtracted lineshapes with Lorentzians using a non-linear least-squares fitting routine. The intensity was taken to be the integrated area under the curve obtained by the fit. Fig. 3 shows the experimental data and the Lorentzian fit of the 440.082 nm line from the 23,229.991 cm^{-1} level. We have previously demonstrated that the determination of relative intensities (branching ratios) from fits to fluorescence spectra is model independent, therefore the use of Lorentzian lineshapes, a good approximation of the instrumental response of the system, is acceptable. [22].

3.1. Experimental parameters

Experimental parameters which could affect the measured Nd II atomic branching ratios were studied including the ambient gas

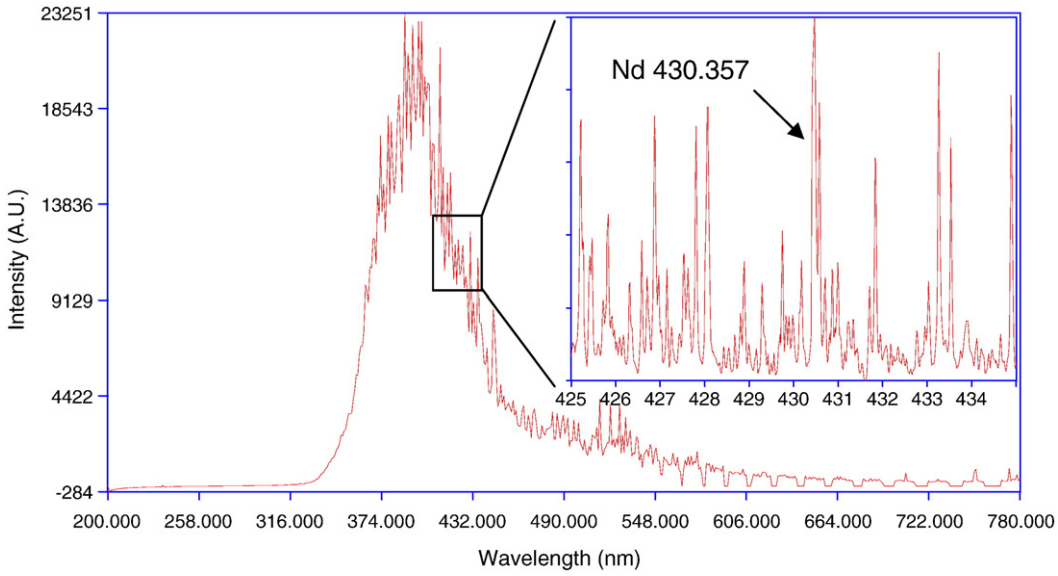

Fig. 2. LIBS Nd spectrum obtained at a pressure of 7.7 mbar, gate delay of 600 ns. The full spectrum ranging from 200–780 nm. (Inset) A zoomed-in detail of the Nd spectrum in the vicinity of the 430.357 nm emission line which is the strongest branch from the 23,229.991 cm^{-1} level studied in this work.

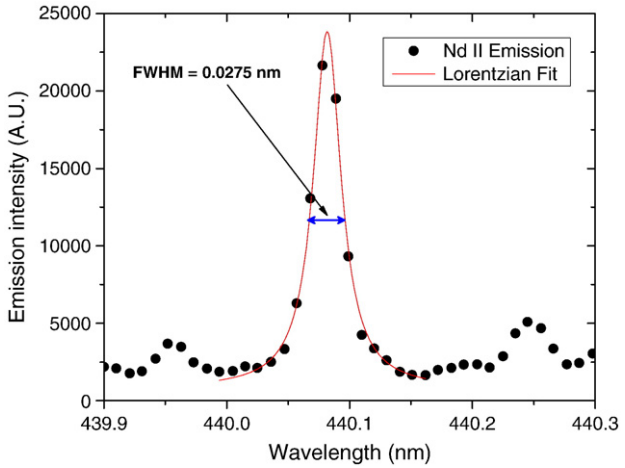

Fig. 3. The experimental data and the fitted Lorentzian of the 440.082 nm line from the 23,229.991 cm^{-1} level. The FWHM of the line is indicated. The resolution of the spectrum and the profile of the spectral lines are determined by the Èchelle spectrometer instrument response.

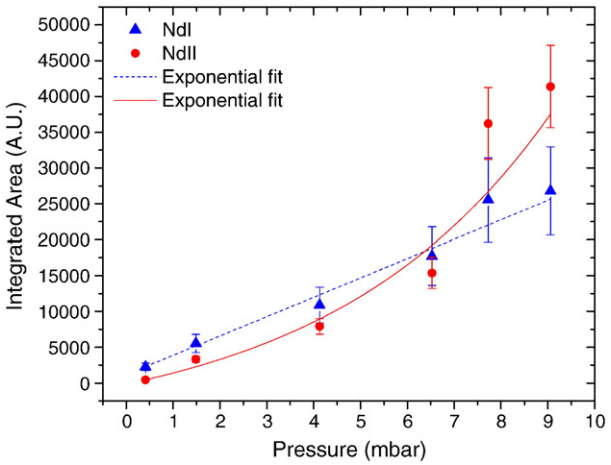

Fig. 4. Absolute emission intensity vs. vacuum chamber pressure for a line of Nd I at 492 nm (triangles) and a line of Nd II at 532 nm (circles). Data have been fitted exponentially.

pressure, gate delay, as well as the number of clean pulses. Clean pulses are initial laser shots which strike the target causing ablation and plasma sparking to provide a fresh target surface for subsequent pulses from which emission is collected. A single clean pulse was found to be best for producing emission signals with the largest line intensities and minimal background. It was also noted that an increase of clean pulses beyond one shot did not improve spectroscopic data.

LIBS spectra were collected from 0.41 mbar to 1040 mbar. At low pressures it was evident that the plasma plume was able to expand more readily, thereby creating a plasma which was less electronically dense. This less-dense plasma is typically problematic for spectroscopy, in that the number of atomic excitations per unit volume becomes significantly reduced. A reduction in excitation decreases the ability to detect sufficient amounts of spontaneously decaying photons for branching ratio measurements. At larger pressures, however, the plasma is confined to smaller volumes, thus creating an optically dense plasma. This dense plasma plume is capable of causing plasma shielding, thus blocking the incident laser and hindering further sample ablation as well as the corresponding increase of electronic number density. Any significant changes within the plasma's composition could directly affect branching ratio measurements and atomic lifetime measurements as well. A pressure between extrema which optimized key parameters was determined to be 7.7 mbar in an argon buffer gas environment. A graph of the resulting integrated emission intensity versus vacuum chamber pressure for a line of Nd I at 436.357 nm and a line of Nd II at 536.147 nm is shown in Fig. 4. The data have both been fit by an exponential growth curve. Although the Nd I data look fairly linear at this delay time, studies of intensity vs. pressure at other, later delay times showed a more clear exponential growth behavior. Therefore an exponential growth function was used for all delay times. The error bars were obtained by calculating the standard deviation of 20 identical spectra.

At a pressure of ~7.7 mbar the plasma plume took on an ovular shape with height and width dimensions of approximately 1.4 cm and 1.0 cm respectively. Because of the large plume size, it was not possible to image the entire plasma onto the core of the multimode fiber. After demagnification through the light collection optics and given an optical fiber diameter of 600 μm, the plasma image in the image plane of the fiber was approximately four fiber-core diameters in height. This corresponded to the ability to image four sections of the plasma independently, but not simultaneously. This is shown in Fig. 5.

Which section of the plasma plume was observed had an effect upon the measured branching ratios and their accuracy. The major parameters which were investigated were emission intensity, signal-to-noise ratio, and the measured Einstein *A*-coefficients and their discrepancy with previously reported *A*-coefficients [4,11,19]. The bottom-most region (region 4) of the plasma plume had signal intensities which were of the smallest magnitude (~500 A.U.) and largest percent discrepancy (~33%); this is not surprising given the density of the plasma. Region 3, the next section above the bottom, yielded stronger signal intensities, ~5000 A.U., which were still small with respect to the continuum background. Region 3 also had a poor *A*-coefficient percent discrepancy compared to those previously reported in other works, approximately 19.7%. Region 2 showed the lowest consistent percent discrepancy (10%) and the highest emission intensity (~9000 A.U.), with the best signal-to-noise. Region 1, the top-most portion of the plasma, revealed a decrease in signal intensity compared with region 3 (~4000 A.U. at delay times ranging from 400 ns to 1000 ns), with rapidly increasing percent discrepancies as a function of delay time (>10%). It was decided that the region of the plasma plume which yielded data best fit for comparison to previous works was the mid-upper region (region 2).

The delay time between the initial ablation laser pulse and observation of the plasma was also studied. A graph of the observed emission intensity as a function of delay time for a line of Nd I at 492.453 nm and Nd II at 536.147 nm is shown in Fig. 6. Although the data look very linear at this specific pressure, studies of intensity vs. delay time at higher pressures showed a very clear exponential decay. Therefore an exponentially decaying function was used to fit data at

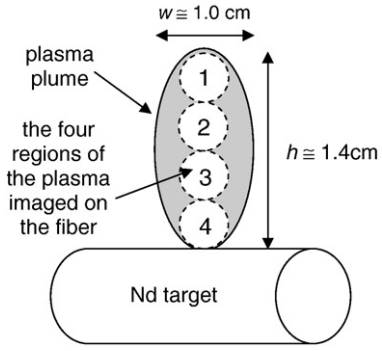

Fig. 5. A schematic of the Nd plasma at low pressures. The spatial extent of the expanding plasma precluded observation of the entire plasma with the light collection optics available. The image of the plasma in the image plane spanned four optical fiber diameters, so four distinct regions of the plasma could be imaged independently, but not simultaneously.

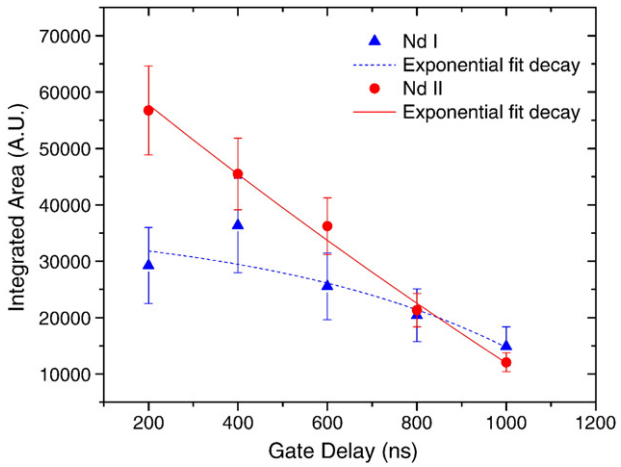

Fig. 6. Absolute emission intensity vs. delay time for a line of Nd I at 492 nm (triangles) and a line of Nd II at 532 nm (circles). Data have been fitted by a decaying exponential.

all pressures, to allow a direct comparison of behavior. The effects of delay time on the measured signal-to-noise ratio and signal-to-background of the observed emission lines were also studied. Lastly, Einstein *A*-coefficients for the eight branches of interest were calculated at various delay times and compared to known values. It was decided that a delay time of 600 ns would be used in all subsequent measurements to maximize emission from the strongest, most obvious emission lines while minimizing the contribution from the broadband background emission and to provide reproducible data most in agreement with previous experiments.

Due to the strong effects that vacuum pressure and gate delay time had on plasma characteristics and therefore the resulting branching ratios, a comparison of the *A*-coefficients from the 23,229.991 cm^{-1} level measured in this work and the author's previous work with Li et al. [4] at the University of Western Ontario was performed. The average percent difference between the Einstein *A*-coefficients of the four strongest branches obtained in the current work and the LIF data from UWO as a function of both argon pressure and ICCD gate delay time is shown in Table 1. In this table, shading is used to indicate agreement, with darker shading indicating closer agreement and lighter shading indicating the largest average percent difference. From this study it was decided that a pressure of 7.7 mbar and a delay time of 600 ns yielded the best average *A*-coefficient agreement with all other reported values. In the pressure range from 4.1 to 9.0 mbar the four averaged *A*-coefficients yielded the best percent discrepancies. At pressures outside of this range the *A*-coefficients deviated further from reported values. This result (sub-10 mbar useful pressures) is entirely consistent with previous measurements of branching ratios using laser-induced plasmas [13,15,17,18]. Due to the large atomic similarity of the lanthanides (atomic mass, electron energy-level structure, nuclear structure, etc.), these parameters will most likely be optimal for all other member of the lanthanides, as well as metals or heavier elements, as indicated by the previous work in silver, cadmium, tin, etc.

3.2. Spectral response calibration

Due to the need for absolute emission intensities, spectral calibration of the instrumentation was necessary. Each optical component of the LIBS detection system (windows, lenses, fiber, etc.) had a certain spectral response associated with it. Spectral calibration of the system was performed using two external light sources. A deuterium–tungsten lamp with a known spectral output over the entire 200 nm to 840 nm spectral range was used to correct the spectra to account specifically for UV loss in the glass of the lens and microscope objective. Relative attenuation in the near-infrared and visible was negligible. In this way, a spectral efficiency factor $\epsilon(\lambda)$ used to correct the observed branching ratio intensity of every line was created. Measured spectral efficiency factors were confirmed by observing the attenuation and subsequent renormalization of the known emission lines from a well-characterized fiber-coupled mercury argon discharge lamp.

3.3. Einstein A-coefficients

A table showing our measured Nd II *A*-coefficients at a pressure of 7.7 mbar and gate delay 600 ns, for branches originating in the 23,229.991 cm^{-1} level is shown in Table 2. Our reported *A*-coefficients (labeled as WSU) for these eight transitions are in agreement with those from the University of Western Ontario [4], UW-Madison [19], as well as the Lund Institute of Technology [11]. The reported values from Western Ontario and Madison are experimentally determined values, combining measured lifetimes and branching ratios. The values from Lund are semi-empirical, obtained by combining experimentally determined lifetimes with theoretical branching ratios. Deviations in reported *A*-coefficients for branches with relatively small contributions (1% or less) are not surprising given the difficulty of measuring these small branches by all the reported methods.

3.4. Atomic lifetimes

We have initiated experiments which utilize the same apparatus in order to make atomic lifetime measurements in laser-ablated gallium via the cascade-photon-coincidence (CPC) technique. In this technique, atomic lifetimes can be measured by detecting photons emitted from spontaneous decays into and out of a particular level of interest [23–25]. The emitted photons signify (i) transitions from a higher energy level into the state of interest and (ii) transitions from the level of interest into a lower energy state. A careful measurement of the time that elapses between observation of these two photons (referred to as "start" and "stop" photons, as their detection starts and stops the sub-ns resolution coincidence electronics) from a single atom (typically on the order of 1–100 ns) yields the lifetime of that level. Specifically, a histogram constructed from the number of observed decays versus the measured delay time will result in an exponentially decaying curve where the decay time constant is the level's lifetime.

We are constructing an apparatus, shown schematically in Fig. 7 and utilizing the same apparatus as was used in the branching ratio study, to perform single-photon counting on the laser-induced

Table 1
Calculation of the average percent difference between the Einstein *A*-coefficients of the four strongest branches obtained in the current work and the LIF data from UWO [4] as a function of both argon pressure and ICCD gate delay time.

	Pres=0.41 mbar	1.5 mbar	4.1 mbar	5.3 mbar	6.5 mbar	7.7 mbar	9.0 mbar	33 mbar	66 mbar	133 mbar	333 mbar	666 mbar	1040 mbar
Gate delay=200 ns	29.44	20.15	6.28	4.86	14.54	5.08	22.17	116.86	148.12	81.64	80.80	93.13	116.55
400 ns	31.33	10.70	6.81	11.54	14.46	10.13	15.51	93.00	57.20	69.35	63.71	87.93	105.66
600 ns	42.52	14.48	10.08	4.99	14.12	3.59	14.58	51.95	54.68	53.63	57.25	86.02	94.69
800 ns	Not measured	18.70	16.13	11.24	14.28	7.44	8.73	40.19	37.94	48.46	44.24	114.37	76.47
1000 ns	Not measured	35.54	14.65	11.04	12.78	14.32	8.90	94.39	41.22	44.06	76.25	132.84	35.41

Darker shading indicates better agreement.

Table 2
A comparison of the Einstein *A*-coefficients (in units of 10^6/s) for branches originating in the Nd II 23,229.991 cm^{-1} level measured in this work to previously determined values.

Wavelength (nm)	WSU[a]	UWO[b]	UW-Madison[c]	Lund[d]
430.357	43.37 ± 7.25	45.37 ± 1.47	43.70 ± 2.30	44.83 ± 4.48
440.082	7.45 ± 2.35	7.11 ± 0.57	8.60 ± 0.50	3.48 ± 1.04
463.267	1.13 ± 0.35	1.08 ± 0.11	0.94 ± 0.07	2.27 ± 0.68
495.814	2.07 ± 0.70	1.47 ± 0.13	1.55 ± 0.10	1.68 ± 0.51
531.982	14.98 ± 4.50	14.42 ± 1.04	17.20 ± 1.30	16.56 ± 1.66
580.400	4.22 ± 1.33	4.27 ± 0.35	5.90 ± 0.50	4.83 ± 1.45
613.396	1.71 ± 0.61	0.39 ± 0.05	Not observed	Not observed
636.554	0.27 ± 0.10	1.08 ± 0.10	1.03 ± 0.12	0.60 ± 0.30

[a] Wayne State University: this work.
[b] University of Western Ontario: R. Li et al. [4].
[c] University of Wisconsin-Madison: E.A. Den Hartog et al. [19].
[d] Lund Institute of Technology: H.L. Xu et al. [11].

plasma. Two single-photon-sensitive avalanche photodiodes with narrow bandpass interference filters will observe the same region of the plasma via a single set of collection optics and subsequent splitting by a Pellicle beamsplitter. Coincidences will be measured with standard Ortec fast timing electronics, commonly used in nuclear decay coincidence measurements.

We have obtained LIBS spectra from a solid gallium target in a helium environment at atmospheric pressure, as is shown in Fig. 8. Numerous emission lines from both Ga I and Ga II were visible. Inset to Fig. 8 shows the spectral regions in the vicinity of the start and stop transitions for the $4s5p^3P_2$ level. Photons from both transitions (at 541 nm and 633 nm) were observed with excellent signal-to-noise and were unblended with any other nearby transitions, indicating the CPC method may be effective for measuring the lifetime of this level.

4. Conclusions

It has been shown that a laser-induced plasma can be used as a source of ions for making branching ratio measurements originating in energy levels in singly-ionized neodymium. The laser-induced plasma was created in a rarified (1–13 mbar) atmosphere of argon. Einstein *A*-coefficients for branches from a particular level of Nd II were measured in this plasma as a function of buffer gas pressure and observation delay time to optimize these experimental parameters. As well, different spatial regions of the plasma were studied for best agreement with previously determined values. The branching ratios of eight branches from the 23,229.991 cm^{-1} level in Nd II were measured and found to be in excellent agreement with three previously determined values from both experiment and theory.

We have also investigated the use of the cascade-photon-coincidence method for determining the atomic lifetime of the $4s5p^3P_2$ level at 118,727.89 cm^{-1} in singly-ionized gallium utilizing a cascade-photon-coincidence technique. Due to its high excitation energy, this lifetime cannot be measured by more traditional LIF/time of flight experiments. Using a helium environment, a Ga laser-induced plasma was created and the requisite start and stop photons at 541 nm and 633 nm were observed in well-isolated, unblended transitions. A CPC apparatus is currently being constructed to use these transitions to measure the lifetime of the level which has never been measured by any method. The dual-purpose use of this laser-induced plasma apparatus demonstrates the flexibility of this convenient source of highly-excited ions. Such measurements made with laser-induced plasmas will allow significant contributions to be made in the study of stellar atmospheres and nucleosynthesis.

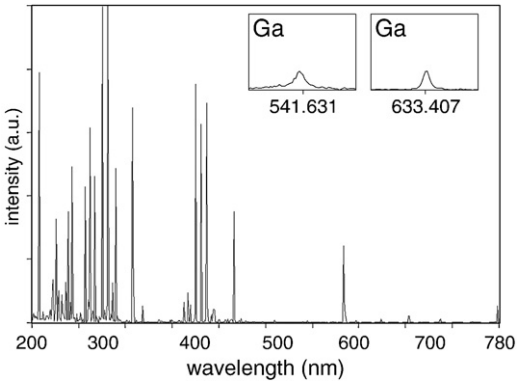

Fig. 8. LIBS spectrum from a Ga target ablated in a helium environment, 200–780 nm. Strong Ga I and Ga II lines are visible. (Inset) The start transition at 541 nm and the stop transition at 633 nm are both visible and unblended in the spectrum of laser-ablated Ga.

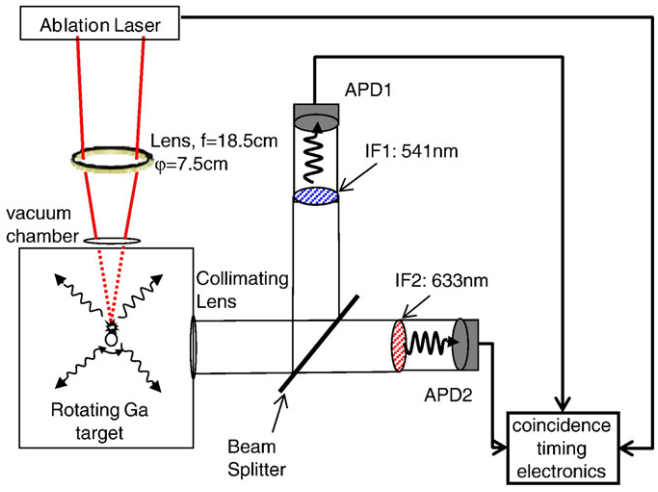

Fig. 7. A schematic of the laser-induced plasma apparatus under construction to perform atomic lifetime measurements via the cascade-photon-coincidence technique. Single-photon-sensitive avalanche photodiodes (APD) with narrow bandpass interference filters (IF) observe the same region of the plasma via a single set of collimating optics and subsequent splitting by a Pellicle beamsplitter. Measurement of the delay between the detection of coincident photons from a single atom (both detected within a narrow pre-set time window) allows a determination of the level lifetime.

References

[1] G.M. Wahlgren, The lanthanide elements in stellar and laboratory spectra, Phys. Scr. T100 (2002) 22–36.
[2] E. Biemont, Recent advances and difficulties in oscillator strength determination for rare-earth elements and ions, Phys. Scr. T119 (2005) 55–60.
[3] G. Wallerstein, J.I. Iben, P. Parker, A.M. Boesgaard, G.M. Hale, A.E. Champagne, C.A. Barnes, F. Kappeler, V.V. Smith, R.D. Hoffman, F.X. Timmes, C. Sneden, R.N. Boyd, B.S. Meyer, D.L. Lambert, Synthesis of the elements in stars: forty years of progress, Rev. Mod. Phys. (1997) 995–1084.
[4] R. Li, S.J. Rehse, T.J. Scholl, A. Sharikova, R. Chatelain, R.A. Holt, S.D. Rosner, Fast-ion-beam laser-induced-flourescence measurements of branching fractions and oscillator strengths in Nd II, Can. J. Phys 85 (2007) 1343–1378.
[5] G. Michaud, Diffusion processes in peculiar A stars, Astrophys. J. 160 (1970) 641–658.
[6] K.C. Smith, Chemically peculiar hot stars, Astrophys. Space Sci. (1996) 77–105.
[7] M.M. Dworetsky, C.M. Jomaron, C.A. Smith, The gallium problem in HgMn stars, Astron. & Astrophys. (1988) 665–672.
[8] A. Jorrisen, Atomic and molecular data for stellar physics: former successes and future challenges, Phys. Scr. T112 (2004) 73–86.
[9] E. Biemont, P. Quinet, Recent advance in the study of lanthanide atoms and ions, Phys. Scr. T105 (2003) 38–54.
[10] G.W.F. Drake (Ed.), Atomic, Molecular, & Optical Physics Handbook, first ed, A.I.P Press, Woodbury, NY, 1996.
[11] H.L. Xu, S. Svanberg, R.D. Cowan, P.H. Lefebvre, P. Quinet, E. Biemont, Theoretical and experimental lifetime and oscillator strength determination in singly ionized neodymium, Mon. Not. R. Astron. Soc. 346 (2003) 433–440.
[12] R.S. Maier, W. Whaling, Transition probabilities in NdII and the solar neodymium abundance, J. Quant. Spectrosc. Radiat. Trans. 18 (1977) 501.
[13] M. Ortiz, J. Campos, R. Mayo, K. Blagoev, G. Malcheva, Possibility of LIBS for transition probabilities determination, S. L. Proc. of SPIE 5830 (2005) 226–230.

[14] A.M. Gonzalez, M. Ortiz, J. Campos, Experimental transition probabilities for lines arising from $5p^2 6s$ configuration of neutral Sb, J. Quant. Spectrosc. Radiat. Transfer 57 (1997) 825–829.
[15] J.A.M. Rojas, M. Ortiz, J. Campos, Determination of transition probabilities of some Sb III lines by time resolved spectroscopy of laser produced plasmas, Phys. Scr. 62 (2000) 364–367.
[16] E. Biémont, H.P. Garnir, P. Palmeri, P. Quinet, Z.S. Li, Z.G. Zhang, S. Svanberg, Core-polarization effects and radiative lifetime measurements in Pr III, Phys. Rev. A 64 (2001) 022503–022508.
[17] J. Campos, M. Ortiz, R. Mayo, P. Quinet, K. Blagoev, Radiative parameters for some transitions in the spectrum of Ag II, Mon. Not. R. Astron. Soc. 363 (2005) 905–910.
[18] H.L. Xu, A. Persson, S. Svanberg, K. Blagoev, G. Malcheva, V. Pentchev, E. Biemont, J. Campos, M. Ortiz, R. Mayo, Radiative lifetime and transition probabilities in Cd I and Cd II, Phys. Rev. A 70 (2004) 1–14 042508.
[19] E.A. Den Hartog, J.E. Lawler, C. Sneden, J.J. Cowen, Improved laboratory transition probabilities for Nd II and application to the neodymium abundances of the Sun and three metal-poor stars, Ap. J. S. 148 (2003) 543–566.
[20] Z.S. Li, H. Lundberg, G.M. Wahlgren, C.M. Sikstrom, lifetime measurements in Ce I, Ce II and Ce III using time-resolved laser spectroscopy with application to stellar abundance determinations of Cerium, Phys. Rev. A 62 (2000) 1–9 032505.
[21] E. Tongnoni, V. Palleschi, M. Corsi, G. Cristoforetti, Quantitative micro-analysis by laser-induced breakdown spectroscopy: a review of the experimental approaches, Spectrochim. Acta Part B 57 (2002) 1115–1130.
[22] S.J. Rehse, R. Li, T.J. Scholl, A. Sharikova, R. Chatelain, R.A. Holt, S.D. Rosner, Fast-ion-beam laser-induced-fluorescence measurements of spontaneous emission branching ratios and oscillator strengths in Sm II, Can. J. Phys. 84 (2006) 723–771.
[23] S.D. Rosner, R.A. Holt, T.J. Scholl, Lifetime measurements using the cascade-photon-coincidence technique with a sputtered-atom source, Phys. Rev. 55 (1997) 3469–3474.
[24] R.E. Mitchell, S.D. Rosner, T.J. Scholl, R.A. Holt, Measurement of the atomic lifetime of Kr II 5p $^4D^0_{7/2}$ and Xe II 6p $^4D^0_{5/2}$ using the cascade-photon-coincidence technique, Phys. Rev. 45 (1992) 4452–4461.
[25] R.A. Holt, F.M. Pipkin, Precision measurement of the lifetime of the 7^3S_1 state of atomic mercury, Phys. Rev. A 9 (1974) 581–584.